Key Engineering Materials
ISSN: 1662-9795, Vol. 1047, pp 299-311

Submitted: 2026-01-19
Revised: 2026-02-16
Accepted: 2026-02-25
Online: 2026-04-13

Advanced FE Modeling for Predicting Component Properties in Additive Manufacturing

Lennart Grüger[1,a*], Tim Sebastian Tübbicke[1,b], Hsuan-Po Huang[1c] and Sebastian Härtel[1,d]

[1]Department Hybrid Manufacturing BTU Cottbus Senftenberg, Konrad-Wachsmann-Allee 17, 03046 Cottbus, Germany

[a*]Lennart.Grueger@b-tu.de, [b]Tim.Tuebbicke@b-tu.de, [c]Huanghsu@b-tu.de, [d]haertel@b-tu.de

Keywords: additive manufacturing, material modeling, FEM-simulation.

Abstract. Wire arc directed energy deposition (WA-DED) is a cost-efficient additive manufacturing process with high deposition rates, yet the prediction of resulting mechanical properties remains challenging due to repeated thermal cycling and associated microstructural changes. Accordingly, this work aims to validate a hardness prediction model for DIN SG2 by Härtel et al. For this purpose, a demonstrator was designed, manufactured, and simulated using a thermal finite element model in the standard software Simufact Welding 2025. Since the DED module of the software used does not adequately represent active interlayer cooling, four substitute models for the convective heat transfer coefficient were implemented and evaluated. In addition, the original hardness prediction model was refined to consider complex path planning, remelting effects and a material-dependent lower temperature limit for tempering or heat treating the material. Using a substitute model that adjusts the convective heat transfer coefficient over time, the improved hardness prediction the adjusted hardness prediction model achieved an accuracy of ±5% for 81 of 88 evaluated measurement points. In order to enable an efficient and reproducible comparison between simulation and experiment, a Python evaluation script was developed. This tool automatically identifies relevant temperature peaks, correlates them with hardness data, creates individual evaluation diagrams and a comparison diagram, and exports all processed data to an Excel file.

Introduction

There is currently a great focus on additive manufacturing (AM) in industry and research [1]. DIN EN ISO/ASTM 52900 describes AM as a manufacturing process that produces components by applying individual layers [2]. The wire arc directed energy deposition (WA-DED) process, also known as wire arc additive manufacturing (WAAM), is one of these promising processes [3, 4]. The advantages of WA-DED compared to other additive manufacturing processes are the relatively high deposition rate and the low purchase costs of the equipment and raw materials [5]. For this reason, the WA-DED process is mainly used in the areas of rapid prototyping, additive repair, rapid tooling, and direct manufacturing [6]. Although the process of deposition welding is well known, the manufacture of WA-DED components remains a challenge [7]. One major challenge in this context is the imprecise predictability of the mechanical properties. This uncertainty results mainly from the process-related multiple over-welding of the individual layers. This makes it impossible to use classic time-temperature transformation (ttt) diagrams, as the repeated application of heat acts like heat treatment on the lower layers. For this reason, Härtel et al. have developed a material model for DIN SG2, which is intended to enable the predictability of the material hardness of a component manufactured using WA-DED [8]. The aim of this work is to validate this model using a demonstrator geometry. For this purpose, the geometry is simulated using the finite element method (FEM) with the standard software Simufact Welding 2025.3 from Hexagon. The demonstrator is manufactured under industry-like conditions, on the GEFERTEC Arc 605 available at the Hybrid Manufacturing Department, and the hardness values are determined. Another challenge is the increase in production times as component volumes rise, with the interlayer time representing a main factor [9]. This is

necessary to bring the interlayer temperature between 200°C and 300°C and to ensure process-safe processing of the material. In order to reduce these interlayer times, the demonstrator is actively cooled with compressed air during breaks. This cooling system is integrated into the equipment used. However, this active air cooling is currently not represented realistically enough in the simulation software. This makes it difficult to predict the temperature-time curves and thus the resulting mechanical properties. Accordingly, this paper proposes several substitute models that are intended to reduce or even eliminate this delta.
Due to the greater complexity of the demonstration geometry compared to the welded wall used by Härtel et al. for hardness model initialization, minor adjustments to the initial hardness model are necessary. Finally, a Python script is used to compare real and simulated data in order to validate the model.

Materials and Methods

Materials.

The demonstrator is made from AWS A5.18 wire (Hermann Fliess & Co. GmbH, Duisburg Germany) with a diameter of Ø = 1.2 mm on a substrate plate (200 x 150 x 18 mm³) made of 1.4404 (316L) and a base plate (AISI 1045) for attaching the substrate plate and holding the thermocouple (TC). The composition of the materials can be found in Table 1. The production setup is visualized in Fig. 1.

Table 1. Chemical composition of the materials used in % weight.

Component	C	Mn	Si	Cu	Fe	P	S	Cr	Mo	Ni	N
Wire (AWS 5.18)	0.06-0.13	1.4-1.6	0.7-1.0	≤0.3	Rest						
Substrat (316L)	max. 0.03	max. 2.0	max. 1.0			max. 0,045	max. 0.03	16.5-18.5	2.0-2.5		max. 0.1
base plate (AISI 1045)	0.42-0.5	0.5-0.8				max. 0.03	max. 0.035	max. 0.4	max. 0.1	max.0.4	

The unalloyed welding wire and the stainless-steel substrate plate are assumed to mix. Accordingly, the first layers are expected to exhibit hardness values that do not correspond to the standard hardness values of SG2. However, this mixing effect should no longer have any influence on the hardness after a few layers.

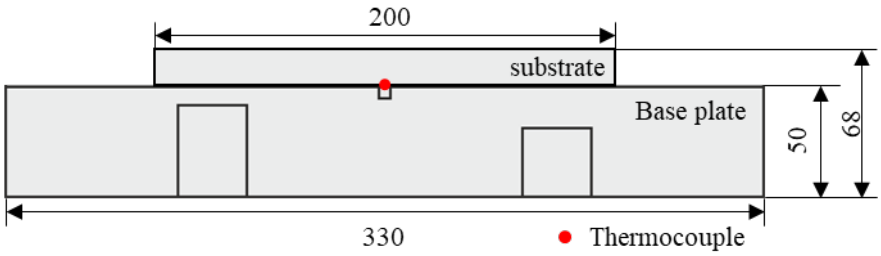

Fig. 1. Schematic visualization of the experimental setup.

Methods. Manufacturing of the demonstrator

Since the model developed by Härtel et al. was based on a welded wall, the aim of this study is to validate the model using a complex demonstrator geometry. For this purpose, various elements were combined in a tower. This tower was manufactured in three steps. First, a cylindrical base body (2.1) with a height of 125 mm and a diameter of 50 mm was welded on. This was then expanded in volume by tilting the machining table in the upper area, creating a 20 mm high flange (2.2) with a diameter of 100 mm. A model of the university library of the BTU Cottbus-Senftenberg, the so-called “Informations-, Kommunikations- und Medienzentrum” (IKMZ), with a height of 50 mm (2.3), was placed on this flange, see Fig. 2.

Fig. 2. Picture of the university library (left) [10]and completed demonstrator (right).

In contrast to the cylinder and the flange, the IKMZ was not manufactured in a spiral shape (3.a). Instead, a hybrid path planning (3.b) consisting of a contour path and a meander band were used, see Fig. 3.a & 3.b. Accordingly, the edge area of a layer was constructed first before it was filled in a meandering pattern. For all partial geometries, the starting point was automatically rotated 30 mm by the CAM software 3DMP to avoid one-sided super elevation. After each layer, the component was actively cooled with compressed air by a cooling system integrated next to the welding unit, see Figure 3.c.

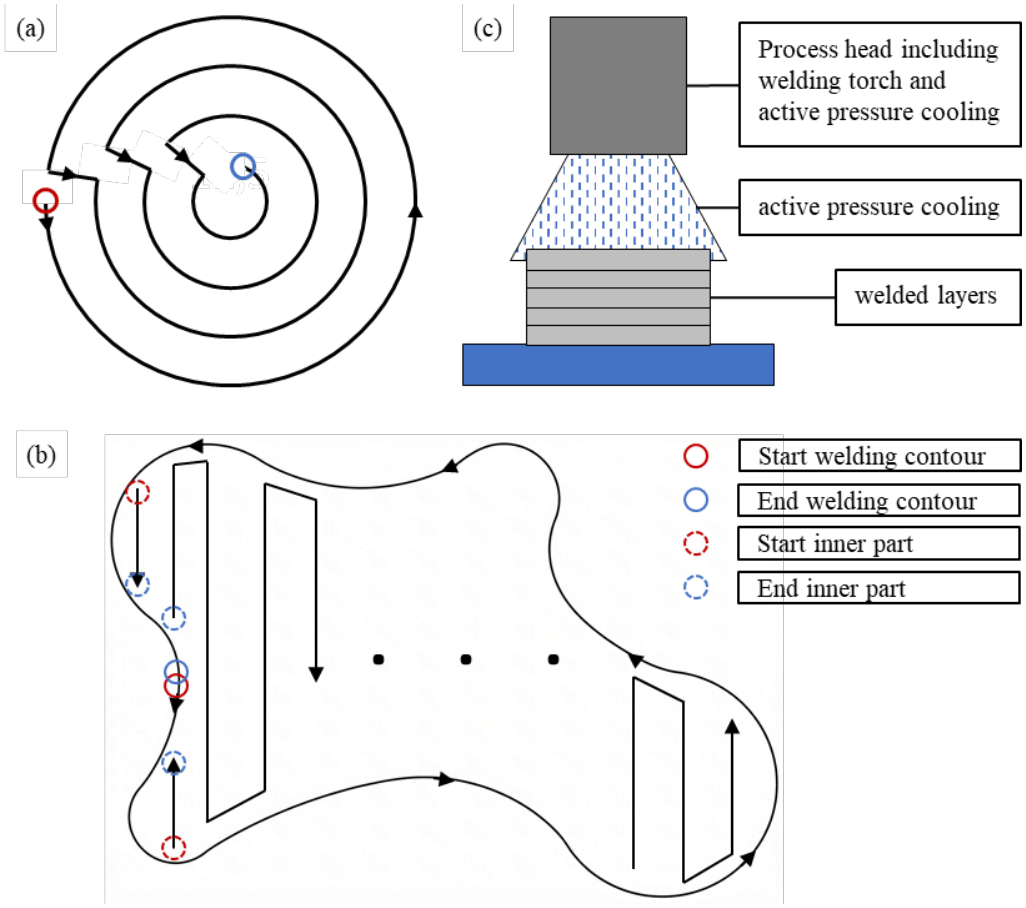

Fig. 3. Schematic overview of the manufacturing strategies (a & b) and the active cooling (c).

This function is used in industrial applications to control cooling in a targeted way and reduce production times. The GEFERTEC Arc 605 is available at the department and was used for the manufacturing process. For the comparison between the actual process and the simulation, a

thermocouple was attached under the substrate plate and the corresponding temperature was recorded during cylinder production. The manufacturing parameters used are shown in Table 1.

Table 2. Process parameters for demonstrator manufacturing.

Parameter	Value
Weld speed	40 [cm/min]
Wire feed rate	4 [m/min]
Mean electric voltage	14.6 [V]
Mean electric current	144 [A]
Interlayer temperature (measured optically using built-in technology)	150 [°C]
Stickout	15 [mm]
Gas / Average shielding gas flowrate	M21-ArC-18 / 15 [l/min]

Methods. FEM simulation.

The FEM simulation was performed using the standard software Simufact Welding 2025.3 available at the Department of Hybrid Manufacturing. For this purpose, all layers of the additive manufacturing process were inserted individually in the form of the machine G-code. Each of these welding layers is assigned the corresponding geometry layer at the corresponding layer height. For the simulation, a mesh must be created. For this purpose, so-called sheet meshes were generated for all simulated geometries (cylinder, flange and IKMZ) using MSC APEX 2025.1 software. For this purpose, the sheet mesher first meshes the upper side of the workpiece with square elements. The volume mesh was then generated by extending these squares into hexahedral elements [11]. The user can select the respective layer thickness. In this work, the layer thickness was assumed to be identical for each geometry for the sake of simplicity. Accordingly, there are 66 layers in the z-direction for the cylinder, five for the flange, and 29 for the IKMZ model. The flange was simplified to 50 individual weld seams. These are rotated by 60° in the simulation, which was equivalent to the angle of rotation of the tilting table. Figure 4 shows the FE model on the left and the corresponding mesh as well as the thermocouple in the cross-section on the right.

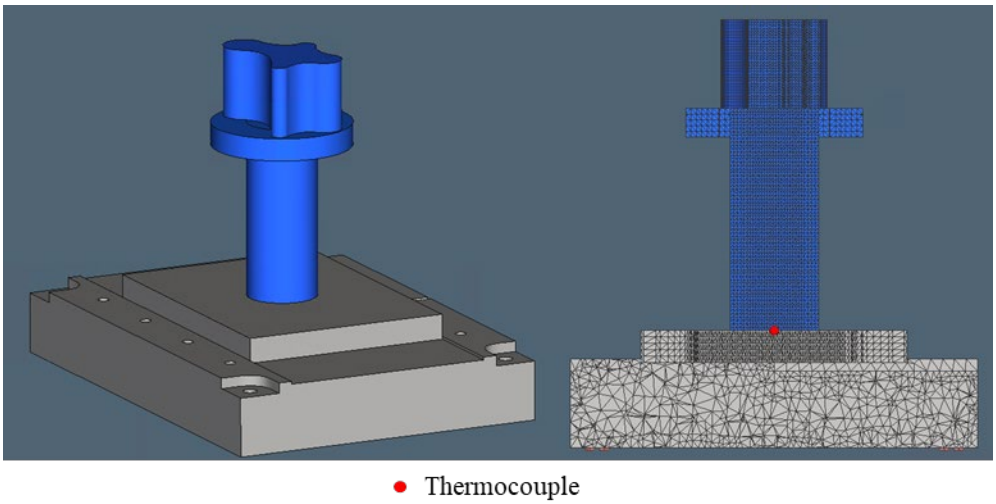

Fig. 4. Visualization of the FE model (left) and its mesh as well as the thermocouple (right).

Finally, measurement points, known as particles, were inserted into the center of each layer and at the edge of the flange in order to evaluate the simulated temperature development in each layer and at the edge of the demonstrator. Another essential particle was modeled under the substrate plate to enable a comparison of the simulation with the thermocouple. For the comparison of the simulation with the sample, it is necessary to analyze the temperature history of individual points within the simulated demonstrator. This was done by selecting the particles that were previously introduced. These can be exported in a .csv file. Subsequently, the expected hardness is calculated according to the model by Härtel et al. using a Python script.

Methods. Evaluation of hardness.

In order to measure hardness, the demonstrator was cut in half and divided into several segments (see Fig. 5) before non-corrosive sample preparation was carried out. The hardness tests were performed using a calibrated model of the DuraScan 70 testing machine from ZwickRoell GmbH & Co KG. For this purpose, a measurement was taken in the low force range HV1 with a test force of 9.807 N. The distance between two measuring points was 0.45 mm. This was determined by dividing the average layer height of 1.8 mm by four, so that the average hardness of a layer was calculated from a total of five measuring points with three measured values each. In this way, a reliable analysis of the hardness distribution within a layer can be performed.

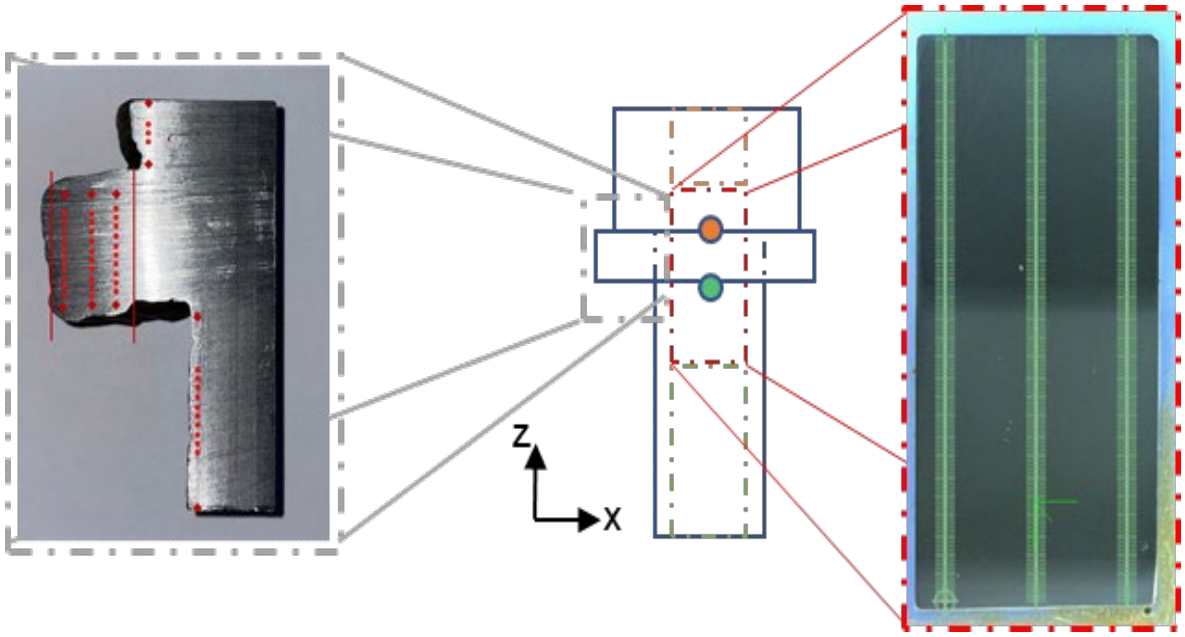

Fig. 5. Idealized demonstrator with extracted and tested segments.

Results

Hardness measurement.

The hardness measurement was carried out as described in Method section. Some measuring points were lost due to the separating edges, reducing the number of measuring points from a calculated 1,248 to 1,183. Furthermore, the measuring points of layers one (324 HV) and two (233 HV) were not considered, as the deviation from the other measuring points suggests that they were mixed with the 316L substrate plate. However, this is not considered by the initial hardness calculation model. Figure 6 shows the hardness distribution of the samples as taken from the demonstrator, and a detailed view of the hardness distribution in the middle and the edge segment.

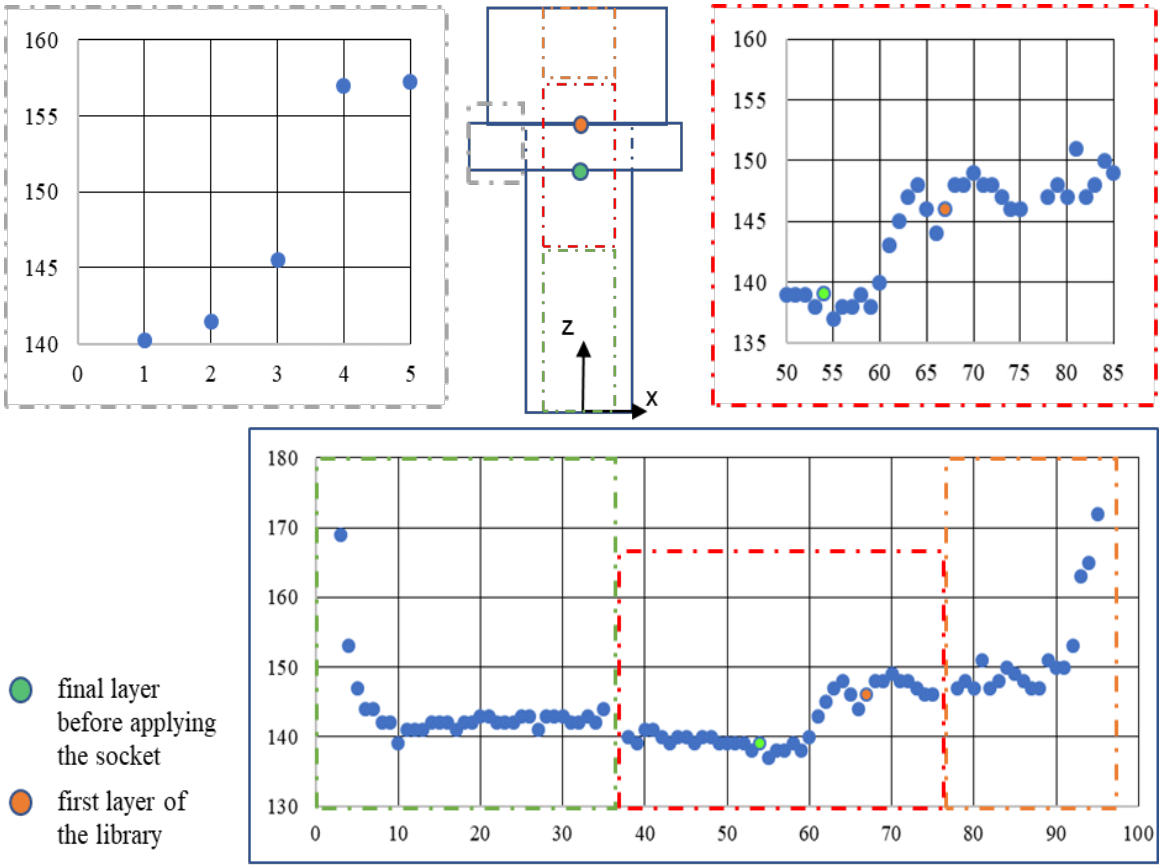

Fig. 6. Visualization of the hardness distribution, and the corresponding sampling areas.

This shows that the rapid cooling in the first layers and the absence of heat treatment in the last layers results in a kind of "bathtub curve". The first layer included in the evaluation develops a hardness of around 170 HV, while the last two layers develop harnesses of 172 HV and 165 HV. In the layers in between, multiple welding cycles reduce the hardness. Due to the constant interlayer temperature, the hardness in the lower segment (green) of the cylinder stabilizes in a narrow range between 139 HV and 146 HV. In the first half of the middle segment, the hardness continues to decrease. After the start of the flange, the hardness fluctuates slightly but tends to increase. This is followed by further hardening of the demonstrator. The reason for this is assumed to be the hybrid path strategy of the IKMZ and the smaller number of weld overlaps or heat cycles. In addition, the division of the material application into contour and internal structure leads to more frequent interruptions of the welding process. This reduces the cooling times, which leads to hardening of the material. The asymmetrical shape of the IKMZ and the rotating starting points result in different welding path courses, which lead to different energy inputs and cooling times. This explains the fluctuating hardness curve.

Adjustment of the simulation.

As described in the methods section, air cooling was performed by the system after the application of each layer. This requires an adjustment of the convective heat transfer coefficient (h) in the Simufact Welding software. There are two main options for performing this adjustment. The first option is to adjust the convective heat transfer over time, and the second option is to adjust it based on the temperature. These adjustment options result in a total of four substitute model options, see Figure 6.

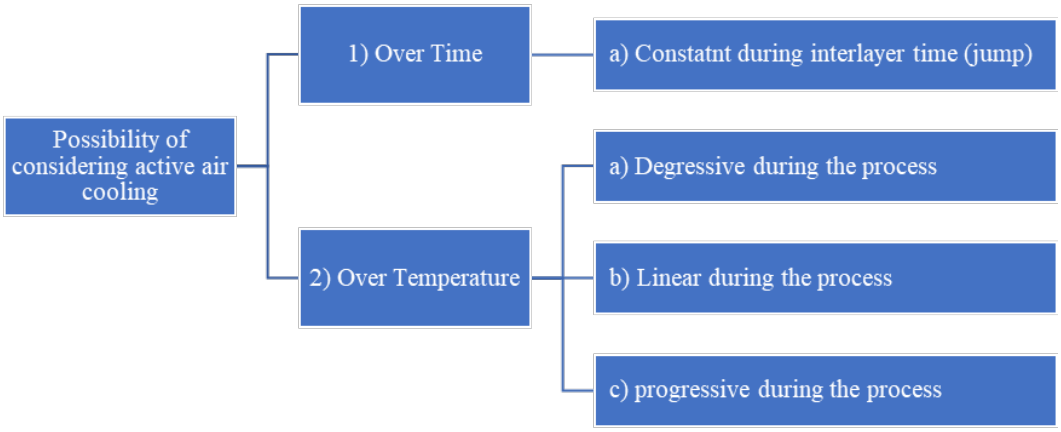

Fig. 7. List of possible substitute models for considering active air cooling.

Assuming that the integrated air-cooling system cools at the same air pressure after each layer, the first replacement model is obtained for adjustment over time. In this model, the convective heat transfer coefficient is adjusted to 300 W/m²*K during the break times, because of the active cooling. This results in the abrupt change in the coefficient shown in Figure 8.

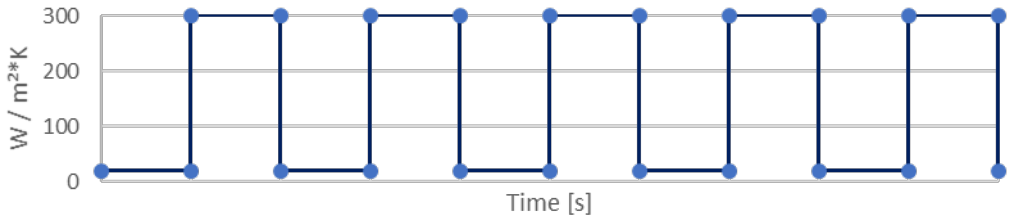

Fig. 8. Extract of Convective heat transfer coefficient of the substitute model 1a).

However, this is not optimal, as the welding unit and thus the compressed air cooling moves upwards with increasing component height, and the influence on the lower layers decreases over time and does not remain constant. This can also be seen in the comparison of the particle under the substrate plate with the real thermocouple, see Fig. 9.

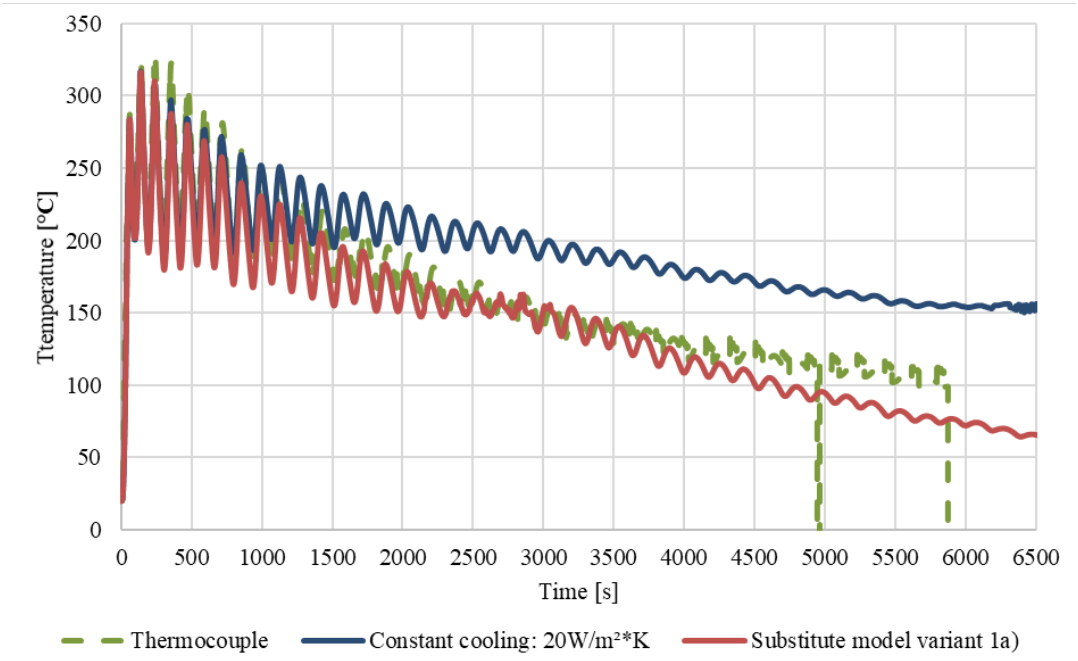

Fig. 9. Comparison of Substitute model 1a) with the thermocouple and the default settings of Simufact Welding.

The analysis shows that the cooling according to the substitute model a) initially reflects the experimental data quite accurate. However, as the process time and respectively component's height increases, the correspondingly decreasing influence of air cooling on the lowest layers can no longer be represented realistically. Accordingly, substitute model 1a) underestimates the temperature in the lower layers with increasing process duration while the default model overestimates the temperature. For the substitute models in which the convective heat transfer coefficient is plotted over temperature, there are essentially three possibilities. These include a degressive (2a), a linear (2b) and a progressive (2c) curve of the coefficient. These are shown in Fig. 10.

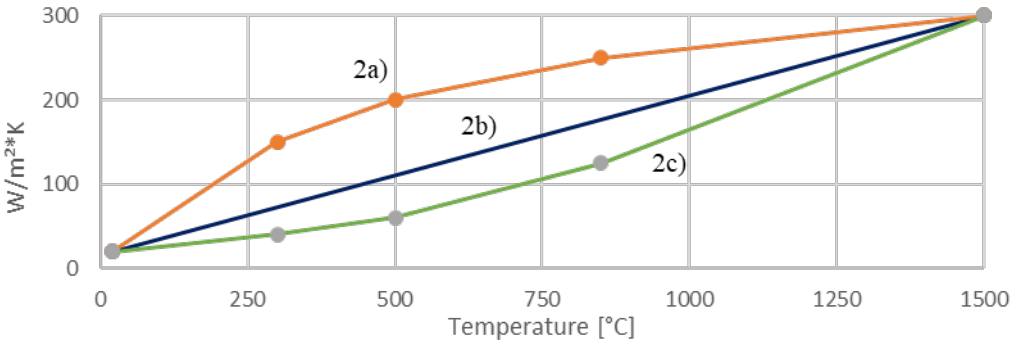

Fig. 10. Extract of Convective heat transfer coefficient of the substitute model 2a)-c).

However, in this setting, cooling also occurs during the application of the material, which also influences the result. A comparison of the individual substitute models with the thermocouple is shown in Fig. 11.

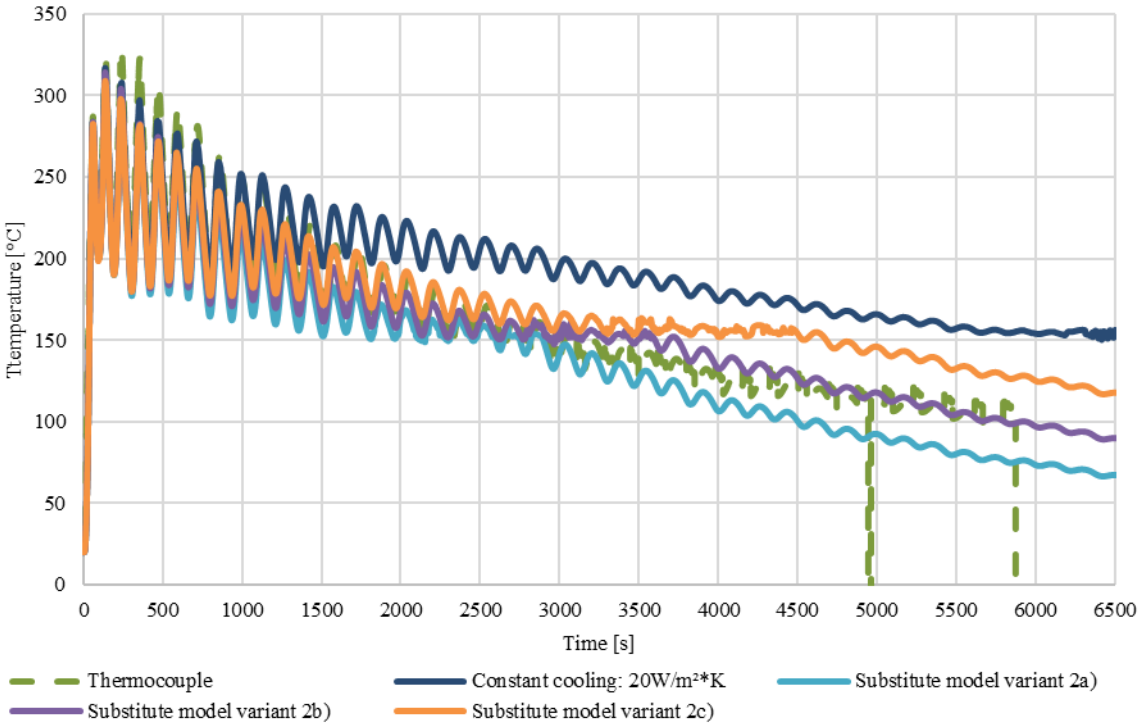

Fig. 11. Comparison of the output of the different replacement models 2a)-c) with the thermocouple and the default settings of Simufact Welding.

The analysis of the different replacement models shows that, at the start, the temperature measured in the experiment is slightly underestimated in all models. However, over the course of the calculation, there are varying degrees of deviation depending on the substitute model.
The substitute models 2a) to c) are effective not only during breaks, but also during material application, depending on the temperature. As a result, model 2a), which simulates a degressively increasing air cooling over the temperature, underestimates the temperature with increasing

component height to a similar extent as substitute model 1a). Model 2c) depicts a progressively increasing air cooling curve depending on the temperature and overestimates the temperature accordingly above a certain component height. A linear approximation, as in substitute model 2b), on the other hand, fluctuates around the experimentally determined hardness with increasing component height and diverges less.
In the result the substitute models 1a) and 2b) fit the experimental data the best. Accordingly, these data are used for the further calculation.

Adjustment of the hardness calculation model.

The investigation of the hardness values in comparison to the expected hardness values from the original model by Härtel et al. revealed a need for adjustment. Deviating from the model by Härtel et al., cooling rates between 850 °C and 500 °C were determined from the last peak above 850 °C in the temperature-time curve. This results in a hardness calculation that can be represented mathematically by Eq. 1:

$$\mathrm{HV_{final}} = \mathrm{HV_{ini}}\left(\mathrm{F}\left(\dot{\mathrm{T}}_{850-500}\right)\right) - \Delta\mathrm{HV}\left(\mathrm{F}\left(\mathrm{E_{thermisch}}\right)\right) \quad (1)$$

This adjustment was necessary because, unlike the manufactured wall used by Härtel et al., the spiral-shaped material application results in several temperature peaks in one layer. Depending on the starting point of the respective weld seam, these increase the temperature peaks in such a way that renewed heat input above 850°C occurs and a new austenitization must be assumed. The correlation between the resulting initial hardness and the cooling rate can be described analytically by a quadratic equation with a very high degree of certainty, see Eq. 2.

$$\mathrm{H_{ini}} = 0{,}0019\,\dot{\mathrm{T}}^2 - 0{,}0188\dot{\mathrm{T}} + 195{,}96\,,\ \mathrm{R^2} = 0{,}98 \quad (2)$$

The formula derived from the analytical approach to describe the change in hardness is a sigmoid function, see Eq. 3.

$$\Delta\mathrm{HV}(\mathrm{F}(\mathrm{E_{thermisch}})) = \Delta\mathrm{HV}(\mathrm{A}) = \frac{51{,}75}{1+\exp\left[-0{,}000333\cdot(\mathrm{A}-13807)\right]} + 1{,}21 \quad (3)$$

This is suitable for modeling the initially slow decrease in hardness at low thermal energy inputs, followed by a steep increase in the transition range and finally a plateau. In addition, there are asymptotically fixed upper and lower limits. In this way, both the maximum hardness reduction of approximately 53 HV measured for SG2 by Härtel et al. as well as the physical lower limit of 0 HV [7]. In contrast, a simple quadratic regression would yield unrealistic, infinitely falling or rising values with increasing energy inputs.
In addition, the model considers the change in hardness (ΔHV) resulting from repeated heat input during subsequent welding processes, based on Härtel et al. The last peak in the austenitizing range above 850 °C is used to calculate the initial hardness. The repeated heat input leads to a reduction in hardness and results from the integrated area below the temperature curve, which results from the heat input of the subsequent layers. The range below 300 °C is no longer considered. The reason for this deviation from the initial model is that tempering below 300°C has no effect on the microstructure of the processed material. Accordingly, the high importance of a realistic consideration of active cooling and the cooling rates thus influenced is also clearly evident. If these cooling rates are calculated incorrectly, errors can occur, especially in limit value cases. For example, heat cycles could be incorrectly considered as complete remelting because the interlayer temperature was calculated higher than it actually was, and the primary temperature of 850 °C was incorrectly exceeded in the subsequent heat cycle. Furthermore, if the cooling rates are underestimated, lower initial hardening values could be calculated, or more heat treatment cycles then appropriate could be considered because the lower limit of 300 °C was incorrectly not reached. This would lead to a miscalculation of the final hardness.
The evaluation was performed using an automated Python script, which was optimized with the help of ChatGPT. This script is particularly important for evaluating the large amounts of data. Due to the size of the demonstrator and the resulting high number of layers, manually evaluating each individual

particle would be extremely time-consuming. In addition to the selection of the primary temperature (850 °C) and secondary temperature (500 °C), the script enables the automated input of .csv files for the temperature curves, as exported from Simufact Welding, and the experimentally determined hardness values as a table (particle number; experimentally determined hardness). Furthermore, it is possible to evaluate only selected particles. Due to the spiral-shaped build-up strategy, there are some cases where several temperature peaks occur in one layer. These are automatically clustered into layers and a preselection is made for the user. In the preselection of the peaks to be used for evaluation, the last peak above the defined peak temperature (default 850°C) is preselected. The user can accept this preselection or manually adjust the selection if justified. The cooling rate is then calculated between the selected peak and 500°C, and the initial hardness is calculated according to Härtel et al. Furthermore, the area under the curve until a value of 300°C is integrated and this area is used as equivalent for the heat energy input to calculate the hardness reduction ΔHV. For the visualization of the evaluation, the font and font size as well as the language (English/German) can be selected. All information used to calculate the simulated hardness, as well as the results, are then displayed in the plot. These plots are made for each particle. Figure 12 shows representative particles 33 located in the center of the cylinder (left) across the entire height of the cylinder in build orientation, and particles 65 located in the cylinder at intermediate height of the flange (right). These are reduced to the essential information on the x-axis and cut off after the third peak below 300 °C. In addition, a comparison plot between experimentally determined hardness and simulated hardness is generated. Based on the test data, an error indicator range can be plotted around the graph. This includes the option of integrating a “very good fit” (here +-1%) and an acceptable fit (here +-5%). The hardness values determined using the model are assigned to the respective tolerance range and the number of “very good,” “acceptable,” and “out of tolerance” fits are output. In addition, the simulated hardness values are colored green, orange, or red. Correspondingly, the simulated hardness is calculated. Finally, all plots and an Excel file with all reference information are output and saved to a previously selected storage location with a previously selected name.

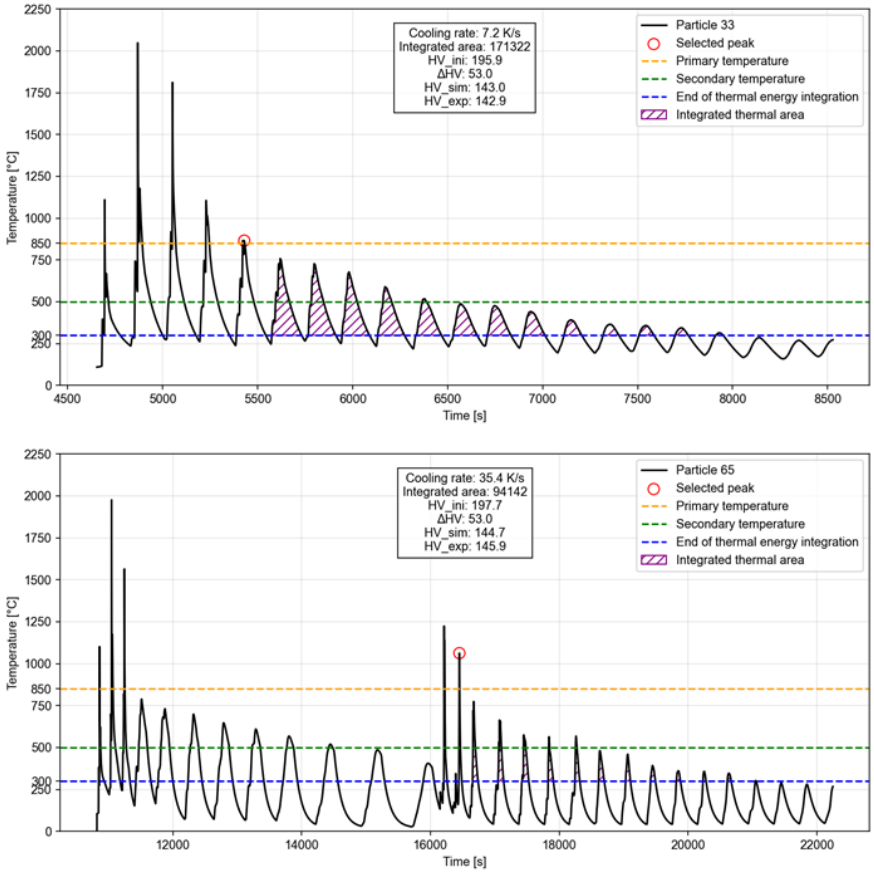

Fig. 12. Example of the calculations based on particle 33 and 65.

The temperature curves and calculation results illustrate that the adjustments in the model also reliably reflect the reheating of the inner cylinder to over 850°C caused by the application of the flange. This results in a deviation of 1.2 HV from the actual measured value for the hardness value of particle 63. Furthermore, the temperature curves already predicted in the initial model by Härtel et al. can still be reliably reproduced. Accordingly, particle 33 shows a deviation of 0.1 HV between the modeled and experimentally determined hardness.

Comparison of adjusted simulation and sample data.

The various replacement models deliver results with varying degrees of accuracy. Figure 13 shows a comparison of the experimentally determined hardness values with the results modeled hardness using default settings as well as the substitute models 1a) and 2b). The first two particles from the first two layers were not evaluated due to material mixing with the substrate plate. Furthermore, the last particle was not evaluated because it is not considered by the model. Due to the fact, that no experimental data could be assigned to four simulated layers because of the cut edges, this results in an evaluation of 88 particles.

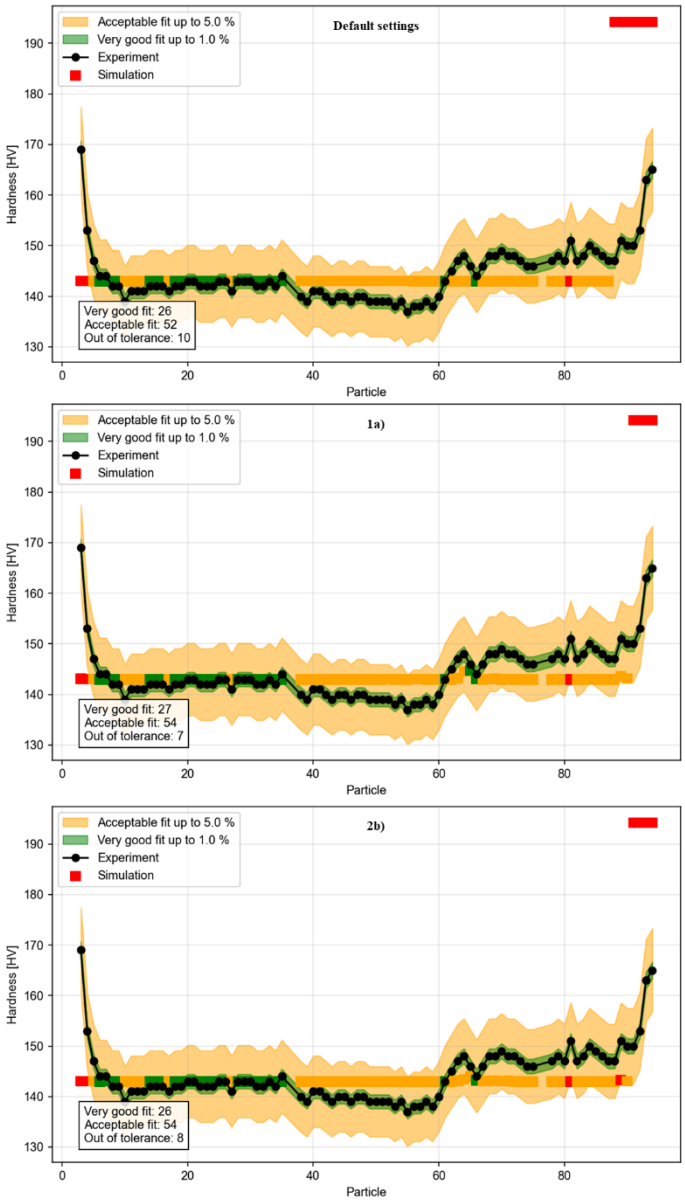

Fig. 13. Comparison of the experimental and the modelled results.

The evaluation of the replacement models in comparison to the actual measured data shows varying degrees of accuracy. Of these, between approximately 89% in replacement model 2b and 92% I

replacement model 1a) are at least within an acceptable fit of +-5% of the experimentally determined hardness values. According to the authors' assumptions, the deviations especially in the edge area are due to the suboptimal fit of the replacement models to the temperature curves determined by measurements.

Summary

The aim of the paper was to manufacture a demonstrator under industrial conditions and to simulate the manufacturing process as accurately as possible using the standard software Simufact Welding 2025.3 in a thermal FE simulation. For this purpose, a demonstrator geometry consisting of a cylinder, a thickening flange, and a model of the university library of the BTU Cottbus-Senftenberg was developed and manufactured. The data resulting from the simulation was used to validate the model for hardness prediction of WA-DED manufactured components by Härtel et al. In order to compare the experiment with the simulation, a thermocouple was attached under the substrate plate. And the hardness of the manufactured Demonstrator was mapped over its height.
Although active air cooling is standard in the system used (GEFERTEC Arc605) to accelerate the cooling time and thus speed up manufacturing, and although such air cooling is common in industry to keep the interlayer temperature between 200 and 300°C for process reliability, the standard software does not represent this cooling process in its DED module without further ado. Accordingly, four substitute models were proposed in this paper. Essentially, there are two ways to deviate from the standard setting of a constant convective heat transfer of 20W/mm²K. One is by adjusting the coefficient over time and the other is by adjusting it over temperature.
The first substitute model adjusts the convective heat transfer coefficient over time. Accordingly, the coefficient is adjusted during the known pause times to address air cooling. However, this means that the influence of air cooling on the lower component layers in the simulation does not decrease even as the component height increases. Accordingly, the simulation underestimates the temperature compared to the actual measured temperature. The remaining three models adjust the coefficient degressively, linearly, or progressively over temperature. However, the simulation also includes the effect during material application in the calculation and does not only cool during the pause times, which also means that the simulated temperature does not fully reproduce the measured temperature.
In addition to the substitute models, the initial model had to be expanded due to the more complex geometry and the associated spiral shape (cylinder and flange) as well as hybrid path planning (IKMZ). Accordingly, the last peak above 850 °C is considered the primary temperature. Furthermore, the integration of thermal energy for calculating the hardness reduction by tempering the resulting structure is now only carried out up to a temperature of 300 °C, as the influence below this temperature is no longer present for the AWS 5.18 used. These adjustments make it possible to consider the subsequent remelting of the material inside the cylinder due to the later weld-on of additional material, which is represented in this case by the flange.
Due to the substitute models and the adjustments to the hardness prediction model, it was possible to model 81 of 88 particles with an accuracy of +-5% using the time-dependent model of coefficient adjustment. With linear adjustment over temperature, the result was 80 of 88 particles.
In order to evaluate the data, a Python script was created. This makes it possible to evaluate the 88 particles in just a few seconds and display them in individual plots as well as in a comparison plot with the measured values. Furthermore, the temperature peaks to be evaluated and the limit temperatures for melting and solidifying can be selected. In addition, an Excel file containing all evaluated data is generated. This greatly facilitates the evaluation and represents a significant time saving.

Forecast

Based on the adjustments to the original model for predicting hardness and the replacement models, the hardness values have already been modeled to an acceptable degree. However, due to the limited possibilities for reproducing active air cooling in Simufact welding's DED module, the pause times

would have to be known in advance in order to adjust the contact heat flow coefficient in advance. Accordingly, it is not possible to accurately predict the resulting hardness values unless the deviation caused by the linear approximation over the temperature is accepted.
The future goal is to model the active air cooling between the layers as a function of the height of the component. This would be another important step toward actively controlling the cooling times and thus the mechanical properties of the components, as well as optimizing production time.

References

[1] J. Bobke, T. Russack, und J. Weinhold, Hrsg., Potenziale und Herausforderungen der Additiven Fertigung: Gesellschaft – Wirtschaft – Wissenschaft und Transfer. in FOM-Edition, FOM Hochschule für Oekonomie & Management. Wiesbaden: Springer Fachmedien Wiesbaden, 2025. doi: 10.1007/978-3-658-45141-7.

[2] „DIN EN ISO/ASTM 52900:2022-03, Additive Fertigung_- Grundlagen_- Terminologie (ISO/ASTM 52900:2021); Deutsche Fassung EN_ISO/ASTM 52900:2021“, Beuth Verlag GmbH, Berlin, 2022. doi: 10.31030/3290011.

[3] S. W. Williams, F. Martina, A. C. Addison, J. Ding, G. Pardal, und P. Colegrove, „Wire + Arc Additive Manufacturing“, Materials Science and Technology, Bd. 32, Nr. 7, S. 641–647, Jan. 2016, doi: 10.1179/1743284715Y.0000000073.

[4] S. C. A. Costello, C. R. Cunningham, F. Xu, A. Shokrani, V. Dhokia, und S. T. Newman, „The state-of-the-art of wire arc directed energy deposition (WA-DED) as an additive manufacturing process for large metallic component manufacture“, International Journal of Computer Integrated Manufacturing, Bd. 36, Nr. 3, S. 469–510, Jan. 2023, doi: 10.1080/0951192X.2022.2162597.

[5] C. Schmid, „Konstruktive Randbedingungen bei Anwendung des WAAM-Verfahrens“, in Konstruktion für die Additive Fertigung 2019, R. Lachmayer, K. Rettschlag, und S. Kaierle, Hrsg., Berlin; Heidelberg: Springer Vieweg, 2020, S. 203–222. doi: 10.1007/978-3-662-61149-4_13.

[6] R. Lachmayer und R. B. Lippert, „Grundlagen“, in Entwicklungsmethodik für die Additive Fertigung, R. Lachmayer und R. B. Lippert, Hrsg., Berlin, Heidelberg: Springer Berlin Heidelberg, 2020, S. 7–20. doi: 10.1007/978-3-662-59789-7_2.

[7] M. Seifi, A. Salem, J. Beuth, O. Harrysson, und J. J. Lewandowski, „Overview of Materials Qualification Needs for Metal Additive Manufacturing“, JOM, Bd. 68, Nr. 3, S. 747–764, Jan. 2016, doi: 10.1007/s11837-015-1810-0.

[8] S. Härtel, J. Szyndler, M. Pakdel Sefidi, und R. Jäger, „Prediction of the evolution of material properties during the AM process based on the FEM simulation and experimental results“, in Materials Research Proceedings, Materials Research Forum LLC, Mai 2024, S. 40–49. doi: 10.21741/9781644903131-5.

[9] Y. Lei, J. Xiong, und R. Li, „Effect of inter layer idle time on thermal behavior for multi-layer single-pass thin-walled parts in GMAW-based additive manufacturing“, Int J Adv Manuf Technol, Bd. 96, Nr. 1–4, S. 1355–1365, Apr. 2018, doi: 10.1007/s00170-018-1699-1.

[10] L. Mösle, „Umbau der BTU-Bibliothek trotz Denkmalschutz – wie das geht“. [Online]. Verfügbar unter: https://www.lr-online.de/lausitz/cottbus/uni-in-cottbus-umbau-der-btu-bibliothek-trotz-denkmalschutz-wie-das-geht-78149145.html.

[11] Hexagon AB (Publ), Simufact Welding 2025.1 Handbuch. Hexagon AB (Publ).